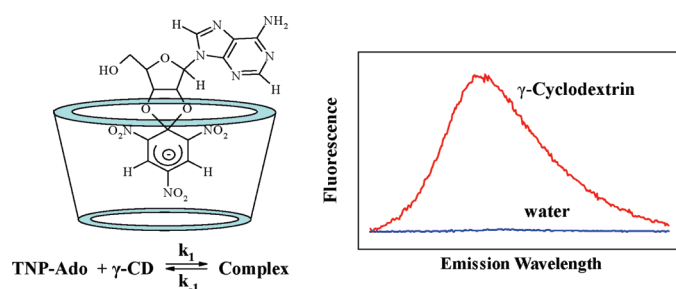


Fluorescence Enhancement of a Meisenheimer Complex of Adenosine by  $\gamma$ -Cyclodextrin: A Thermodynamic and Kinetic InvestigationThomas K. Green,<sup>\*,†</sup> Luc Denoroy,<sup>‡,§</sup> and Sandrine Parrot<sup>§</sup>

<sup>†</sup>Department of Chemistry & Biochemistry, Institute of Arctic Biology, University of Alaska Fairbanks, Fairbanks, Alaska 99775, <sup>‡</sup>Laboratoire de Neuropharmacologie, EAC CNRS 5006, Université Lyon 1, F-69373 Lyon Cedex 08, France, and <sup>§</sup>NeuroChem, Institut Fédératif des Neurosciences de Lyon, Université de Lyon, F-69373 Lyon, France

tkgreen@alaska.edu

Received February 26, 2010



The fluorescent properties of a trinitrophenylated Meisenheimer complex of adenosine (TNP-Ado) in water were examined in the presence of  $\alpha$ -,  $\beta$ -, and  $\gamma$ -cyclodextrins (CDs). The TNP-Ado complex exhibits minimal fluorescence in water, whereas addition of 10 mM  $\alpha$ -CD,  $\beta$ -CD, and  $\gamma$ -CD enhances fluorescence by factors of 2, 7, and 110, respectively. The large enhancement by  $\gamma$ -CD is attributed to its larger hydrophobic cavity, which is able to accommodate the TNP moiety of TNP-Ado.  $^1\text{H}$  NMR spectra demonstrate 1:1 stoichiometry of the complex, which undergoes slow exchange on the NMR time scale.  $^1\text{H}$  NMR and 2D ROESY spectra reveal substantial interaction of the TNP hydrogens with  $\gamma$ -CD. Equilibrium constants were determined by fluorimetry from 10 to 20 °C by nonlinear curve fitting. Fluorescence is temperature dependent, with maximum fluorescence increasing with decreasing temperature. Complexation is exothermic with large negative entropy, consistent with formation of a tight complex between TNP-Ado and  $\gamma$ -CD. Rate constants and activation parameters for both complexation and dissociation were determined by a combination of fluorimetry and 2D NMR exchange spectroscopy (EXSY).

## 1. Introduction

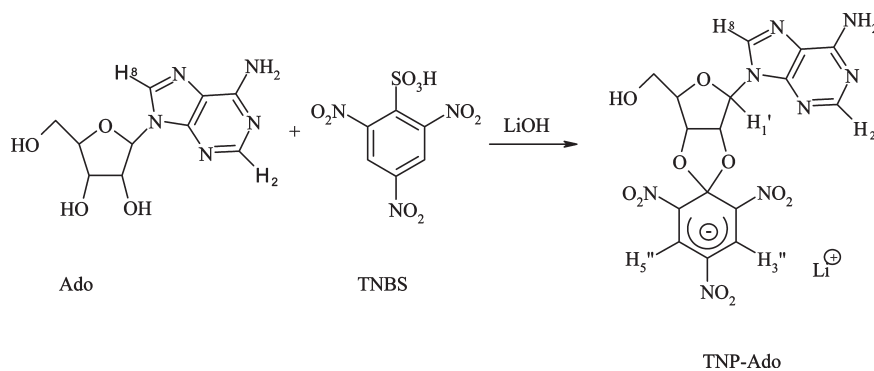
Adenosine is an important neuromodulator with both excitatory and inhibitory properties, and its extracellular concentration in mammalian brain ranges from nanomolar to micromolar concentrations. Adenosine is involved in locomotion, sleep, and respiration, as well as neuroprotection during hypoxia and ischemia.<sup>1–3</sup> Separation and detection of adenosine in biological

matrices is usually accomplished by absorbance methods using either capillary electrophoresis or liquid chromatography.<sup>4,5</sup> Alternatively, adenosine can be derivatized with chloroacetaldehyde to form a fluorescent product that is amenable to these separation techniques.<sup>6,7</sup> Shortcomings of the fluorescence technique include high temperatures (80–95 °C) for derivatization which can lead to degradation at long times, and the requirement of a low wavelength laser ( $\lambda_{\text{max}}$  275 nm), often not available in many laboratories. A goal of our research is to develop a new capillary electrophoresis/laser-induced fluorescence detection method for adenosine and related nucleotides such as ATP.

(1) Porkka-Heiskanen, T. *Ann. Med. (Helsinki)* **1999**, *31*, 125–129.  
(2) Boison, D. *Neuroscientist* **2005**, *11*, 25–36.  
(3) Pedata, F.; Pugliese, A. M.; Coppi, E.; Popoli, P.; Morelli, M.; Schwarzschild, M. A.; Melani, A. *Immunol., Endocr. Metab. Agents Med. Chem.* **2007**, *7*, 304–321.  
(4) Akula, K. K.; Kaur, M.; Bishnoi, M.; Kulkarni, S. K. *J. Sep. Sci.* **2008**, *31*, 3139–3147.  
(5) Ng, M.; Blaschke, T. F.; Arias, A. A.; Zare, R. N. *Anal. Chem.* **1992**, *64*, 1682–1684.

(6) Katayama, M.; Matsuda, Y.; Shimokawa, K. I.; Tanabe, S.; Kaneko, S.; Hara, I.; Sato, H. *J. Chromatogr., B: Biomed. Sci. Appl.* **2001**, *760*, 159–163.  
(7) Tseng, H. C.; Dadoo, R.; Zare, R. N. *Anal. Biochem.* **1994**, *222*, 55–58.

## SCHEME 1. Synthesis of TNP-Ado from Adenosine (Ado) and Trinitrobenzenesulfonic Acid (TNBS) at pH 9.5



Azegami and Iwai showed that the diol function of the ribose moiety of adenosine (Ado) can be easily trinitrophenylated (TNP) to form a Meisenheimer complex (TNP-Ado) as shown in Scheme 1.<sup>8</sup> Hiratsuka and Uchida also showed that the Meisenheimer complex of the nucleotide ATP, weakly fluorescence (quantum yield  $2.0 \times 10^{-4}$ ) in water, exhibits marked fluorescence enhancement upon binding to proteins.<sup>9,10</sup> Thus TNP-ATP has been used to investigate binding interactions between nucleotides and various proteins with over 400 papers published from 1987 to 2003.<sup>11</sup> In addition to binding state, the fluorescence of TNP-ATP is also sensitive to solvent, viscosity, and pH.<sup>12</sup> The loss of fluorescence at low pH has been attributed to the ring-opening of the Meisenheimer dioxolane ring,<sup>12</sup> a process that has been fully characterized by NMR spectroscopy for the adenosine derivative.<sup>13</sup> The Meisenheimer complexes of TNP-Ado and TNP-ATP show two absorbance maxima at  $\sim 410$  and  $\sim 476$  nm, with a single fluorescence emission maximum in the range of 530–560 nm.<sup>14</sup>

The high sensitivity of TNP-ATP fluorescence to microenvironment suggested to us that TNP-Ado fluorescence might be substantially enhanced in the presence of cyclodextrins thus allowing Ado in biological matrices to be analyzed by capillary electrophoresis/laser-induced fluorescence detection, employing cyclodextrin in the background electrolyte. Cyclodextrins possess a hydrophobic cavity into which either the adenine base and/or TNP moiety can bind. The size of the CD cavity can be varied ( $\alpha$ -,  $\beta$ -, and  $\gamma$ -CD) and the CD can be chemically modified to optimize host–guest interaction, leading to maximum enhanced fluorescence. A number of studies demonstrate

that cyclodextrins can significantly enhance fluorescence of molecules that exhibit low quantum yields.<sup>15–28</sup>

To test this hypothesis, we examined the steady-state fluorescence behavior of TNP-Ado in the presence of  $\alpha$ -,  $\beta$ -, and  $\gamma$ -CD. TNP-Ado can be prepared and purified from its one-step reaction with trinitrobenzenesulfonic acid (TNBS) under basic conditions as shown in Scheme 1.<sup>9</sup> It is stable in water for weeks. We demonstrate that its fluorescence is particularly sensitive to the size of the hydrophobic cavity of the cyclodextrin ( $\alpha$ -,  $\beta$ -, or  $\gamma$ -CD). Maximum fluorescence enhancement is achieved with  $\gamma$ -CD. <sup>1</sup>H NMR spectra demonstrate 1:1 stoichiometry of the complex, which undergoes slow exchange on the NMR time scale. 2D NMR EXSY (Exchange Spectroscopy) analysis and steady-state fluorescence measurements allow an estimation of the equilibrium constants, rate constants, and activation parameters for complexation and dissociation. The results are consistent with the formation of a *tight* inclusion complex of TNP-Ado and  $\gamma$ -CD, which results in large negative enthalpy and entropy of complexation. We suggest that the enhanced fluorescence is attributed to restricted rotation of the nitro groups upon inclusion into the hydrophobic cavity of  $\gamma$ -CD.

## 2. Results and Discussion

**2.1. Fluorescence Measurements.** The corrected fluorescence spectra of 4  $\mu$ M TNP-Ado in water with 10 mM cyclodextrin are shown in Figure 1. Fluorescence is enhanced significantly in the presence of  $\gamma$ -CD compared to  $\alpha$ -CD and  $\beta$ -CD. From integrated fluorescence intensities (480–620 nm) of aqueous solutions of TNP-Ado (0–4  $\mu$ M) in 10 mM  $\gamma$ -CD, we estimate an enhancement factor of  $\sim 110$  for  $\gamma$ -CD compared to  $\sim 2$  and  $\sim 7$  for  $\alpha$ -CD and  $\beta$ -CD, respectively. Quantum yield ( $\Phi$ ) for TNP-Ado in 10 mM  $\gamma$ -CD was estimated as 0.02 at 476 nm excitation by comparison with fluorescein ( $\Phi = 0.97$ ).

Steady-state fluorescence measurements were carried out on 10  $\mu$ M solutions of TNP-Ado in water at different  $\gamma$ -CD concentrations and temperatures. Corrected fluorescence

- (8) Azegami, M.; Iwai, K. *J. Biochem.* **1964**, *55*, 346–348.  
 (9) Hiratsuka, T.; Sakata, I.; Uchida, K. *J. Biochem.* **1973**, *74*, 649–659.  
 (10) Hiratsuka, T. *Biochim. Biophys. Acta* **1976**, *453*, 293–297.  
 (11) Hiratsuka, T. *Eur. J. Biochem.* **2003**, *270*, 3479–3485.  
 (12) Ye, J. Y.; Yamauchi, M.; Yogi, O.; Ishikawa, M. *J. Phys. Chem. B* **1999**, *103*, 2812–2817.  
 (13) Ah-kow, G.; Terrier, F.; Pouet, M.-J.; Simonnin, M.-P. *J. Org. Chem.* **1980**, *45*, 4399–4404.  
 (14) Hiratsuka, T. *Biochim. Biophys. Acta* **1982**, *719*, 509–517.  
 (15) Burai, T. N.; Panda, D.; Datta, A. *Chem. Phys. Lett.* **2008**, *455*, 42–46.  
 (16) Jalali, F.; Afshoon, A. *J. Fluoresc.* **2008**, *18*, 219–225.  
 (17) Vasquez, J. M.; Vu, A.; Schultz, J. S.; Vullev, V. I. *Biotechnol. Prog.* **2009**, *25*, 906–914.  
 (18) Mesplet, N.; Morin, P.; Ribet, J. P. *Eur. J. Pharm. Biopharm.* **2005**, *59*, 523–526.  
 (19) Catena, G. C.; Bright, F. V. *Anal. Chem.* **1989**, *61*, 905–909.  
 (20) Yang, R.; Li, K. a.; Wang, K.; Zhao, F.; Li, N.; Liu, F. *Anal. Chem.* **2003**, *75*, 612–621.  
 (21) Abdel-Shafi, A. A.; Al-Shihry, S. S. *Spectrochim. Acta, Part A* **2009**, *72A*, 533–537.  
 (22) Baglolle, K. N.; Boland, P. G.; Wagner, B. D. *J. Photochem. Photobiol., A* **2005**, *173*, 230–237.

- (23) Lee, S.-M.; Lee, J.-S.; Kim, J.-M. *Macromol. Symp.* **2007**, *249/250*, 67–70.  
 (24) Liu, W.-l.; Tang, B. *J. Environ. Sci. (Beijing, China)* **2004**, *16*, 829–831.  
 (25) Ramirez-Galicia, G.; Garduno-Juarez, R.; Vargas, M. G. *Photochem. Photobiol. Sci.* **2007**, *6*, 110–118.  
 (26) Stone, M. T.; Anderson, H. L. *Chem. Commun. (Cambridge, U.K.)* **2007**, 2387–2389.  
 (27) Yang, Y.; Yang, X.; Jiao, C.-X.; Yang, H.-F.; Liu, Z.-M.; Shen, G.-L.; Yu, R.-Q. *Anal. Chim. Acta* **2004**, *513*, 385–392.  
 (28) Park, J. S.; Wilson, J. N.; Hardcastle, K. I.; Bunz, U. H. F.; Srinivasarao, M. *J. Am. Chem. Soc.* **2006**, *128*, 7714–7715.

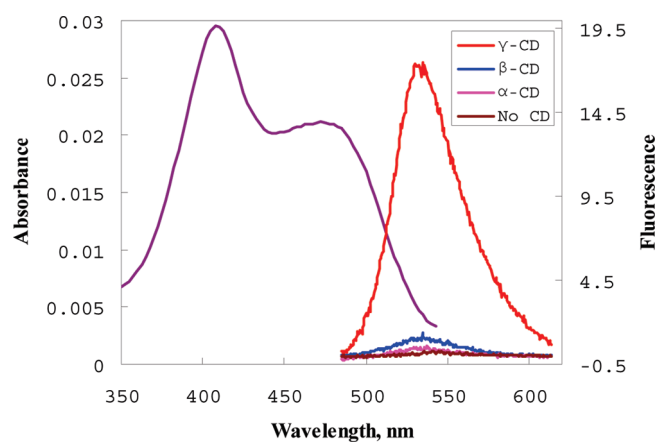


**FIGURE 1.** Absorbance of pure TNP-Ado in water (left) and fluorescence of aqueous TNP-Ado (4  $\mu$ M) and cyclodextrins (10 mM). Excitation for fluorescence was 408 nm.

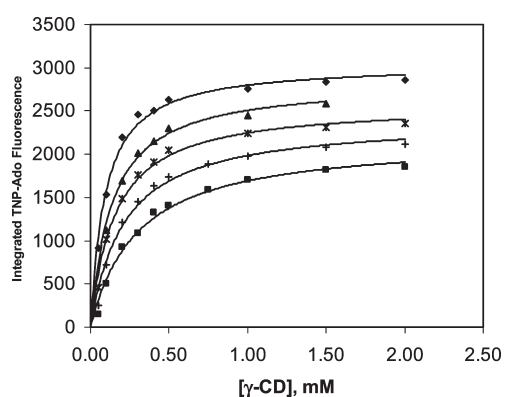


**FIGURE 2.** Integrated fluorescence intensity of TNP-Ado (10  $\mu$ M) as a function of  $\gamma$ -CD concentration:  $\blacksquare$ , 20.0  $^{\circ}$ C;  $+$ , 17.5  $^{\circ}$ C;  $*$ , 15.0  $^{\circ}$ C;  $\blacktriangle$ , 12.5  $^{\circ}$ C;  $\blacklozenge$ , 10.0  $^{\circ}$ C. Excitation was at 408 nm. Emission was collected at 480–630 nm. The solid lines represent the best fit to the experimental data according to a 1:1 stoichiometry.

integrals are plotted against concentration of  $\gamma$ -CD in Figure 2. Fluorescence increases as  $\gamma$ -CD concentration increases as expected. Lower temperatures enhance fluorescence at a given concentration of  $\gamma$ -CD. Maximum fluorescence values ( $F_{\max}$ ) were determined by using 20 mM  $\gamma$ -CD, shown in Table 1, which increase as temperature is lowered. These  $F_{\max}$  values at 20 mM  $\gamma$ -CD are only about 6–20% higher than the fluorescence observed at 2 mM  $\gamma$ -CD, consistent with a leveling off of fluorescence at higher concentrations of  $\gamma$ -CD.

Equilibrium constants were determined by nonlinear least-squares curve fitting of the fluorescence data. We prefer this approach to determining equilibrium constants rather than the classical approach of double reciprocal plots. Specifically, double reciprocal plots place more weight on lower ( $1/\text{intensity}$ ) values.<sup>19</sup> Corrected fluorescence data were fit assuming a 1:1 stoichiometry for equilibrium according to



Equilibrium constants were determined by two approaches. The solid lines in Figure 2 represent the two-parameter fit to the experimental data up to 2 mM  $\gamma$ -CD, where both  $K$  and the saturation fluorescence,  $F'_{\max}$ , are

outputs of the analysis. All curves had an  $R^2$  value of better than 0.994, in support of a 1:1 stoichiometry for inclusion of TNP-Ado into  $\gamma$ -CD. The calculated  $F'_{\max}$  values, shown in Table 1, closely agree with experimental  $F_{\max}$  values. Equilibrium constants were also calculated by using a one-parameter fit with the experimental  $F_{\max}$ . The agreement in calculated  $K$  values is excellent, demonstrating that the fluorescence data over the entire concentration range are consistent with 1:1 stoichiometry. Double reciprocal plots were also highly linear over the entire concentration range (see the Supporting Information, Figure S-16), consistent with 1:1 stoichiometry.<sup>29</sup>  $^1\text{H}$  NMR spectra discussed below also support a 1:1 stoichiometry.

**2.2.  $^1\text{H}$  and 2D ROESY NMR Spectra.**  $^1\text{H}$  NMR spectra of the aromatic regions of TNP-Ado in  $\text{D}_2\text{O}$  are shown in Figure 3. The intense singlets in the 8.08 and 8.21 ppm region (no CD) are assigned to H-2 and H-8 of the adenine base of TNP-Ado, respectively (see Scheme 1). The doublets at 8.52 and 8.57 ( $J = 3.0$  Hz) are assigned to two  $\text{H}_{\text{TNP}}$  resonances (H-3'' and H-5'') of the TNP moiety, which are anisochronous. All four hydrogen resonances experience a downfield shift in the presence of  $\alpha$ -CD and  $\beta$ -CD with virtually no peak broadening. In contrast, the hydrogen resonances are significantly broadened in the presence of  $\gamma$ -CD, with a significant upfield shift of one  $\text{H}_{\text{TNP}}$  resonance, as well as a significant downfield shift of the H-2 resonance of the adenine base. The broadening is indicative of a strong interaction of TNP-Ado with  $\gamma$ -CD in comparison to  $\alpha$ -CD and  $\beta$ -CD.

The  $^1\text{H}$  NMR spectra of the  $\gamma$ -CD (3.5–4.0 ppm) in the absence and presence of TNP-Ado are shown on the top of Figure 4. It is well-known that H-3 and H-5 of the D-glucose unit of CDs are internal and are directed toward the hydrophobic cavity of the CD, whereas H-2 and H-4 are directed externally.<sup>30</sup> The two H-6 hydrogens are positioned on a rim of the CD. The H-3, H-5, and two H-6 resonances appear in the downfield region (3.7–4.0 ppm) in the absence of TNP-Ado, whereas the H-2 and H-4 resonances appear in the upfield region, with integrations of 4:2 for these two regions, respectively. The spectrum in the presence of 1 equiv of TNP-Ado is substantially broadened, with integrations of 3:3 for the two regions. Thus a single H resonance has shifted into the upfield region upon complexation with TNP-Ado. Resonance  $\text{H}_3$  can be identified in the downfield region as it appears as a distinct triplet, and it is probable that H-5 is shifted into the upfield region, although the spectra do not allow an unambiguous assignment. The corresponding spectra for  $\alpha$ -CD and  $\beta$ -CD showed no substantial changes in their spectra upon TNP-Ado addition (see the Supporting Information, Figures S-3 and S-4).

To investigate further, a 2D ROESY NMR spectrum was acquired for the TNP-Ado: $\gamma$ -CD complex (1:1 ratio) in  $\text{D}_2\text{O}$ , shown in Figure 4. The adenine hydrogen H-2 and H-8 show intense through-space correlations with the downfield region of  $\gamma$ -CD. Both TNP hydrogens show correlation with CD

(29) Although double reciprocal plots have  $R^2$  values  $>0.98$  at all temperatures, a reviewer has pointed out that the data points at low  $[\gamma\text{-CD}]$  (high  $1/[\gamma\text{-CD}]$ ) values of less than 0.2 mM appear to systematically deviate from linearity compared to data points at high  $\gamma$ -CD concentrations. It is suggested that this deviation may be indicative of the presence of a minor complex with a stoichiometry other than 1:1. Notwithstanding, application of the continuous variation method<sup>31</sup> to  $^1\text{H}$  NMR data (see text), which directly integrates the signal attributed to the complex, supports 1:1 stoichiometry for the major complex.

(30) Schneider, H.-J.; Hackett, F.; Ikeda, V. R. *Chem. Rev.* **1998**, *98*, 1755–1786.

**TABLE 1. Equilibrium and Rate Constants for Complexation and Dissociation of TNP-Ado and  $\gamma$ -CD**

temp, °C	$F_{\max}^a$	$K,^b \times 10^{-3} \text{ M}^{-1}$	$F'_{\max}^c$	$K,^c \times 10^{-3} \text{ M}^{-1}$	$\Delta G, \text{ kJ mol}^{-1}$	$k,^d \text{ s}^{-1}$	$k_1,^e \times 10^{-4} \text{ M}^{-1} \text{ s}^{-1}$	$k_{-1},^f \times 10^{-4} \text{ M}^{-1} \text{ s}^{-1}$	$k_{-1},^g \text{ s}^{-1}$
20.0	2300	3.46 ± 0.14	2310 ± 60	3.29 ± 0.32	-19.8 ± 0.3	23.5 ± 0.9	3.70 ± 0.53	3.9 ± 0.5	11.0 ± 0.4
17.5	2430	4.66 ± 0.26	2400 ± 80	4.86 ± 0.55	-20.5 ± 0.3	16.3 ± 0.2	3.64 ± 0.47	3.6 ± 0.5	7.5 ± 0.2
15.0	2600	6.58 ± 0.33	2590 ± 60	6.70 ± 0.64	-21.1 ± 0.3	10.1 ± 0.3	3.07 ± 0.36	3.0 ± 0.3	4.5 ± 0.2
12.5	2870	7.37 ± 0.28	2840 ± 60	6.95 ± 0.60	-21.2 ± 0.3	6.2 ± 0.4	2.08 ± 0.32	2.1 ± 0.3	2.7 ± 0.2
10.0	3120	10.5 ± 0.6	3050 ± 60	11.4 ± 1.1	-22.0 ± 0.3	3.8 ± 0.3	1.85 ± 0.40	1.9 ± 0.4	1.6 ± 0.2

<sup>a</sup>Determined with 10  $\mu\text{M}$  TNP-Ado and 20 mM  $\gamma$ -CD. The values are relative (see Figure 2). <sup>b</sup>Determined by one-parameter nonlinear curve fitting of steady-state fluorescence data with experimental  $F_{\max}$  values. <sup>c</sup>Determined by two-parameter nonlinear curve fitting of steady-state fluorescence data, where both  $K$  and  $F'_{\max}$  are outputs of the calculation. <sup>d</sup>Determined from volume integration of 2D EXSY NMR spectrum and eqs 3 and 4. <sup>e</sup>Calculated from  $k_1 = Kk_{-1}$ . <sup>f</sup>Calculated from  $k_{-1} = k_1/[\gamma\text{-CD}]_{\text{eq}}$ , where  $[\gamma\text{-CD}]_{\text{eq}}$  is calculated from  $K$  and initial NMR concentrations of TNP-Ado (4.0 mM) and  $\gamma$ -CD (2.4 mM). <sup>g</sup> $k_{-1} = k/(X_{\text{complex}}/X_{\text{TNP-Ado}} + 1)$ , where mole fraction  $X$  is obtained from NMR integration

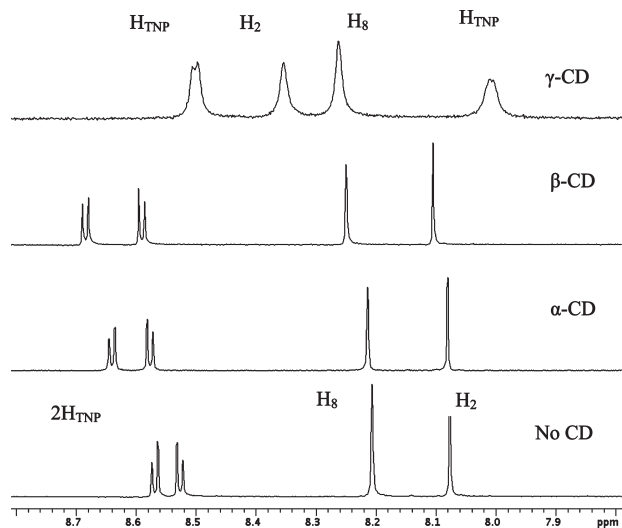


**FIGURE 3.**  $^1\text{H}$  NMR spectra of the aromatic region of TNP-Ado in the absence and presence of cyclodextrins. The ratio of TNP-Ado:CD is 1:1 and the solvent is  $\text{D}_2\text{O}$ .

resonances centered at 3.86 and 3.60 ppm. Although a definitive interpretation of the ROESY spectrum is not possible given the overlap of the CD resonances, the intense crosspeaks clearly point to a strong interaction of TNP-Ado with  $\gamma$ -CD. We hypothesize that it is the TNP moiety that includes into the  $\gamma$ -CD cavity, giving rise to the observed crosspeak correlations. We note that underivatized Ado does not significantly alter the  $^1\text{H}$  spectrum of  $\gamma$ -CD (1:1 ratio). Additionally, the strong *upfield* shift of one of the TNP hydrogens (Figure 3) is consistent with its inclusion into the cavity.

To assess the nature of the exchange process, a series of  $^1\text{H}$  NMR spectra were acquired at 20 °C on solutions in which the ratio of TNP-Ado to  $\gamma$ -CD was systematically varied. The total concentration of TNP-Ado and  $\gamma$ -CD for each solution was constant at 1.0 mM, so that the data are amenable to the Continuous Variation Method for determining stoichiometry of complexation.<sup>31</sup> The aromatic regions of the spectra are shown in Figure 5. The presence of just 10%  $\gamma$ -CD reveals significant broadening and shifting of the downfield TNP-Ado resonance, indicating interaction of  $\gamma$ -CD at the TNP moiety. This resonance merges with the other TNP-Ado resonance at higher  $\gamma$ -CD concentrations. At  $\sim 30\%$   $\gamma$ -CD, four new

aromatic resonances become evident. One TNP resonance is shifted significantly upfield, whereas H-2 is shifted downfield of the H-8 resonance. At a  $\sim 1:1$  ratio, the spectrum simplifies to four relatively broad resonances. Yet higher concentrations of  $\gamma$ -CD do not significantly alter the spectrum.

The  $^1\text{H}$  NMR spectra at less than stoichiometric concentrations of  $\gamma$ -CD are consistent with the existence of an uncomplexed and complexed form of TNP-Ado which undergoes slow exchange on the NMR time scale. Moreover, the spectrum at a 1:1 ratio of TNP-Ado and  $\gamma$ -CD is consistent with a large binding constant for addition of the first equivalent of  $\gamma$ -CD to TNP-Ado. To assess the stoichiometry, the spectra are analyzed according to the Continuous Variation Method<sup>31</sup> for slow exchange in which the relative concentration of complex,  $[\text{TNP-Ado} \cdot \gamma\text{-CD}]$ , was estimated by integration of the well-resolved resonances of the complex,  $\text{H}_{\text{TNP}}$  at 8.0 ppm and  $\text{H}_2$  at 8.35 ppm. The total mole fraction of TNP-Ado in the mixture is then plotted against concentration of the complex. In such a plot, the maximum occurs at a value of  $a/(a + b)$ , where the formula of the complex is  $(\text{TNP-Ado})_a(\gamma\text{-CD})_b$ . The maximum occurs at 0.5 mol fraction TNP-Ado, so  $a = b$  and the stoichiometry of the complex is 1:1 (see the Supporting Information, Figure S-13)

$^1\text{H}$  NMR spectra of the 1:1 TNP-Ado: $\gamma$ -CD mixture were also acquired in the range of 2–60 °C (see the Supporting Information, Figure S-7). At 2 °C, TNP-Ado is predominately complexed by  $\gamma$ -CD. As the temperature is raised, several aromatic resonances broaden to the point of disappearing. At 60 °C, the spectrum simplifies to four aromatic resonances. The results are consistent with a predominately uncomplexed TNP-Ado at 60 °C. The spectral region of the  $\gamma$ -CD resonances was also consistent with this conclusion. The spectrum at 25 °C was reproduced after heating the sample to 70 °C, cooling back to 25 °C, and reacquiring the spectrum (see the Supporting Information, Figure S-8). The reversibility of the spectrum upon heating–cooling demonstrates that the system was initially at equilibrium.

**2.3. 2-D EXSY Spectra.** 2-D EXSY (Exchange Spectroscopy) NMR spectra provide a means of quantitative determination of rate constants for the slow exchange process.<sup>32</sup> 2D EXSY spectra were acquired over a range of mixing times (20–220 ms) and temperatures (10–20 °C) on a  $\text{D}_2\text{O}$  solution of excess TNP-Ado (4.0 mM) with  $\gamma$ -CD (2.4 mM). The aromatic region of a  $^1\text{H}$  NMR spectrum at 20 °C is shown in Figure 6. The mole fraction of uncomplexed ( $X_{\text{TNP-Ado}}$ ) to

(31) Schalley, C., Ed. *Analytical Methods in Supramolecular Chemistry*; Wiley-VCH: Weinheim, Germany, 2007.

(32) Perrin, C. L.; Dwyer, T. J. *Chem. Rev.* **1990**, *90*, 935–967.



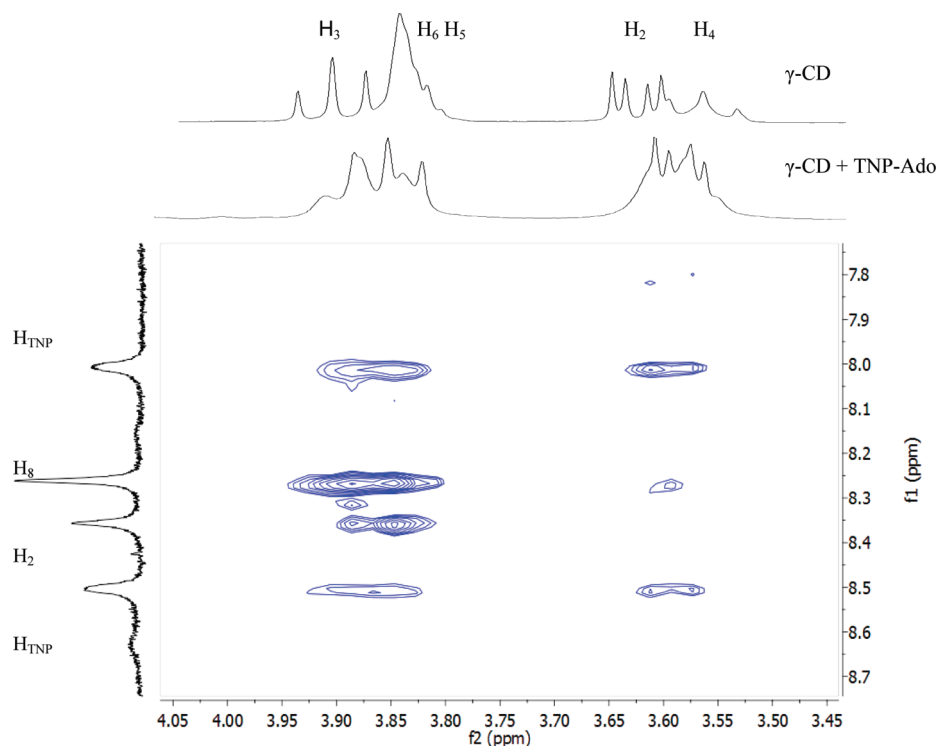


**FIGURE 4.** Partial ROESY NMR spectrum of a 1:1 mixture of TNP-Ado and  $\gamma$ -CD in  $D_2O$ . The top spectrum is  $\gamma$ -CD in the absence of TNP-Ado for comparison.

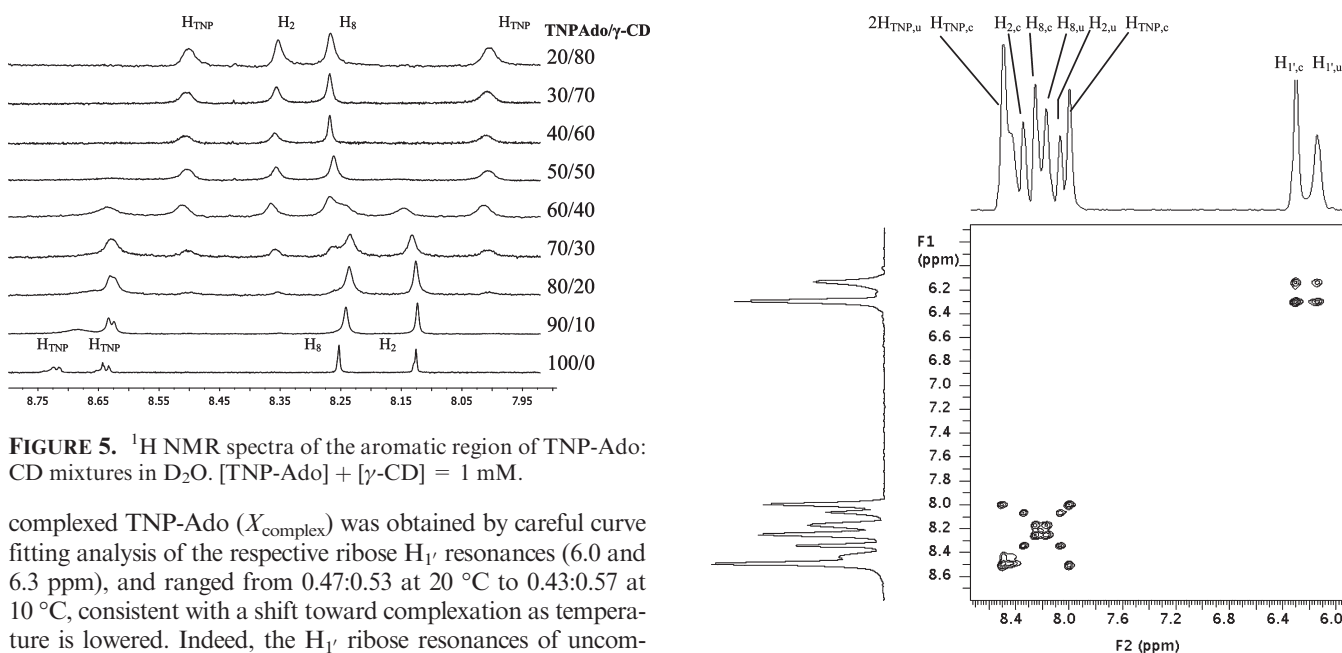


**FIGURE 5.**  $^1H$  NMR spectra of the aromatic region of TNP-Ado:CD mixtures in  $D_2O$ .  $[TNP-Ado] + [\gamma-CD] = 1$  mM.

complexed TNP-Ado ( $X_{\text{complex}}$ ) was obtained by careful curve fitting analysis of the respective ribose  $H_{1'}$  resonances (6.0 and 6.3 ppm), and ranged from 0.47:0.53 at 20 °C to 0.43:0.57 at 10 °C, consistent with a shift toward complexation as temperature is lowered. Indeed, the  $H_{1'}$  ribose resonances of uncomplexed and complexed TNP-Ado were sufficiently intense and well-resolved to allow for reliable volume integration of the diagonal and crosspeaks of the EXSY spectra, as shown in Figure 6. Data were fit according to eqs 3 and 4 in the Experimental Section, where the mixing time  $t_m$  is plotted against the quantity  $\ln[(r + 1)/(r - 1)]$ , shown in Figure 7 for the various temperatures. The slope of the curve yields the rate constant  $k$ , where  $k = k'_1 + k'_{-1}$ , with  $k'_1$  and  $k'_{-1}$  being pseudo-first-order rate constants for complexation and dissociation of the complex. Dissociation is a first order process, presumably, and  $k'_{-1}$  is therefore a true rate constant,  $k_{-1}$ , which can be calculated from

**FIGURE 6.** The downfield region of the 2D EXSY spectrum of a mixture of uncomplexed and complexed TNP-Ado (ratio 0.47:0.53) at 20 °C. Mixing time was 80 ms. The diagonal and crosspeak volumes of the ribose resonances  $H_{1',u}$  and  $H_{1',c}$  at 6.1 and 6.3 ppm, respectively, were integrated to determine rate constants in the 10–20 °C range with use of eqs 3 and 4.

$k$  with a knowledge of the mole fractions of uncomplexed and complexed TNP-Ado obtained from NMR integration ( $k_{-1} = k / (X_{\text{complex}}/X_{\text{TNP-Ado}} + 1)$ ). Rate constants for dissociation with standard errors at the different temperatures are shown

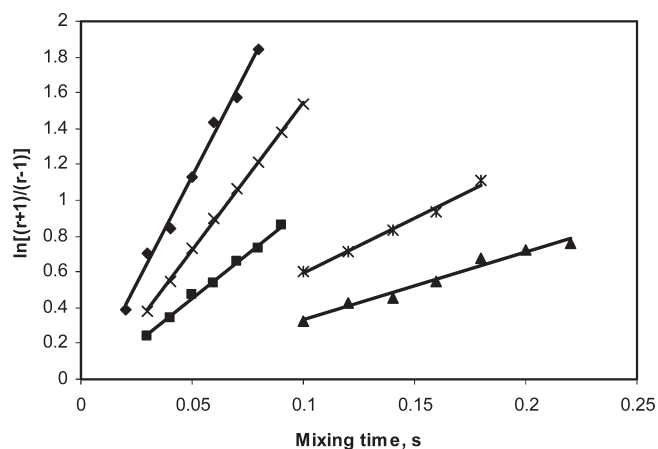


**FIGURE 7.** EXSY data plotted according to eq 3:  $\blacklozenge$ , 20.0 °C;  $\times$ , 17.5 °C;  $\blacksquare$ , 15.0 °C;  $*$ , 12.5 °C;  $\blacktriangle$ , 10.0 °C. Slopes are equal to rate constants  $k = k'_1 + k'_{-1}$ .

in Table 1. The rate constants are consistent with the requirement for slow exchange of  $R_{\text{exchange}} \ll \Delta\nu_{\text{AB}}$ , where  $R_{\text{exchange}}$  is the rate of exchange (1–11 Hz) and  $\Delta\nu_{\text{AB}}$  is the chemical shift difference between the uncomplexed and complexed resonances, in the case of ribose H-1, 0.2 ppm  $\times$  300 Hz/ppm = 60 Hz.

The rate constants were analyzed by using the Eyring equation to obtain activation parameters. A plot of  $\ln(k_{-1}/T)$  vs  $1/T$  yields a straight line, where the slope is  $-\Delta H^\ddagger_{-1}/R$  and the intercept is  $\ln(k_{\text{B}}/h) + \Delta S^\ddagger_{-1}/R$ , where  $\Delta H^\ddagger_{-1}$  is the activation enthalpy,  $\Delta S^\ddagger_{-1}$  is the activation entropy,  $k_{\text{B}}$  is the Boltzmann constant,  $h$  is the Planck constant, and  $R$  is the gas constant.  $\Delta H^\ddagger_{-1}$  was determined as  $131 \pm 4 \text{ kJ mol}^{-1}$  and  $\Delta S^\ddagger_{-1}$  was determined as  $221 \pm 13 \text{ J K}^{-1} \text{ mol}^{-1}$ . The free energy of activation,  $\Delta G^\ddagger_{-1}$ , is then calculated from  $\Delta H^\ddagger_{-1}$  and  $\Delta S^\ddagger_{-1}$  to be  $66 \pm 8 \text{ kJ mol}^{-1}$  at 293 K. Errors for activation parameters were determined from corresponding standard errors in slopes and intercepts.

Equilibrium constants were determined by nonlinear curve fitting (Levenberg–Marquardt algorithm) of steady-state fluorescence measurements on 10  $\mu\text{M}$  TNP-Ado solutions, with  $\gamma$ -CD concentrations ranging from 0.05 to 2.0 mM  $\gamma$ -CD, shown in Figure 2. The equilibrium constants in Table 1 are strongly temperature sensitive, consistent with a highly exothermic process. Van 't Hoff treatment of the constants yield  $\Delta H_{\text{complex}} = -80 \pm 7 \text{ kJ mol}^{-1}$  and  $\Delta S_{\text{complex}} = -204 \pm 25 \text{ J mol}^{-1} \text{ K}^{-1}$  (see the Supporting Information, Figure S-12).

Equilibrium constants ( $K$ ) were used to calculate rate constants for complexation,  $k_1$ , in two ways. First  $k_1 = Kk_{-1}$ , where  $k_{-1}$  is determined from EXSY NMR data. In addition,  $k_1$  determined from EXSY data is a pseudo-first-order rate constant where  $k_1 = k_1[\gamma\text{-CD}]_{\text{eq}}$  and therefore  $k_1 = k_1'/[\gamma\text{-CD}]_{\text{eq}}$ , where  $[\gamma\text{-CD}]_{\text{eq}}$  is the equilibrium concentration of uncomplexed  $\gamma$ -CD.  $[\gamma\text{-CD}]_{\text{eq}}$  was calculated from a knowledge of  $K$  and the initial concentrations of TNP-Ado and  $\gamma$ -CD used in the EXSY analysis (4.0 and 2.4 mM, respectively), assuming a 1:1 stoichiometry. There is good agreement between  $k_1$  calculated by the two methods, as shown in Table 1.

Eyring analysis of the rate constants  $k_1$  afforded the activation parameters for the complexation process. Both kinetic and thermodynamic parameters for the complexation process are summarized in Table 2. The data in Table 2 reveal a highly exothermic complexation ( $\Delta H_{\text{complex}} = -80 \pm 7 \text{ kJ mol}^{-1}$ ) with

**TABLE 2.** Summary of Activation and Thermodynamic Parameters for Complexation and Dissociation of TNP-Ado and  $\gamma$ -CD at 20 °C

$\Delta G_{\text{complex}}$ , $\text{kJ mol}^{-1}$	$\Delta H_{\text{complex}}$ , $\text{kJ mol}^{-1}$	$\Delta S_{\text{complex}}$ , $\text{J mol}^{-1} \text{ K}^{-1}$
$-20 \pm 1$	$-80 \pm 7$	$-204 \pm 25$
$\Delta G^\ddagger_1$ , $\text{kJ mol}^{-1}$	$\Delta H^\ddagger_1$ , $\text{kJ mol}^{-1}$	$\Delta S^\ddagger_1$ , $\text{J mol}^{-1} \text{ K}^{-1}$
$46 \pm 16$	$53 \pm 8$	$25 \pm 28$
$\Delta G^\ddagger_{-1}$ , $\text{kJ mol}^{-1}$	$\Delta H^\ddagger_{-1}$ , $\text{kJ mol}^{-1}$	$\Delta S^\ddagger_{-1}$ , $\text{J mol}^{-1} \text{ K}^{-1}$
$66 \pm 8$	$131 \pm 4$	$221 \pm 21$

large negative entropy of complexation ( $\Delta S_{\text{complex}} = -204 \pm 25 \text{ J mol}^{-1} \text{ K}^{-1}$ ). It is useful to examine these parameters in context of an enthalpy–entropy compensation effect observed for cyclodextrin complexation.<sup>33–35</sup> This effect describes an empirical, linear relationship between  $\Delta H$  and  $T\Delta S$  for complexation of cyclodextrins and guests, according to the equation:

$$T\Delta S^\circ = \alpha\Delta H^\circ + T\Delta S_0^\circ \quad (2)$$

Inoue and Rekharsky have compiled thermodynamic data for more than 1000 data sets and found good linear correlation between the  $\Delta H$  and  $T\Delta S$  values.<sup>34</sup> For the data set for  $\gamma$ -CD, comprising over 60 pairs, the slope of such a plot ( $\alpha$ ) is 0.97 with intercept  $T\Delta S_0^\circ$  of  $15 \text{ kJ mol}^{-1}$ . Our data are consistent with this empirical relationship, as the experimental  $\Delta H^\circ$  value of  $-80 \text{ kJ mol}^{-1}$  yields a calculated  $T\Delta S^\circ$  value of  $-63 \text{ kJ mol}^{-1}$ , in good agreement with the measured value of  $-60 \text{ kJ mol}^{-1}$ .

The magnitudes of  $\Delta H^\circ$  and  $T\Delta S^\circ$  measured for Ado complexation with  $\gamma$ -CD are considerably more negative than those for any data pair compiled by Inoue and Rekharsky for  $\gamma$ -CD.<sup>34</sup> Indeed, of 1000 pairs compiled for all natural cyclodextrins, including  $\alpha$ -CD and  $\beta$ -CD, only a few pairs exhibited  $\Delta H^\circ$  values more negative than  $-70 \text{ kJ mol}^{-1}$ , and only 3 pairs exhibited  $T\Delta S^\circ$  values more negative than  $-60 \text{ kJ mol}^{-1}$ . Thus, we can conclude that  $\Delta H^\circ$  and  $T\Delta S^\circ$  values for TNP-Ado complexation with  $\gamma$ -CD are unusually negative and that complexation is exclusively enthalpy-driven.

The strong inclusion of an anionic guest such as TNP-Ado into a cyclodextrin is not unprecedented. A particularly striking and relevant example is the case of  $\alpha$ -CD complexation to 4-nitrophenol and 4-nitrophenolate, which have binding constants of 210 and  $2300 \text{ M}^{-1}$ , respectively.<sup>33,36</sup> The stronger binding of  $\alpha$ -CD to the anionic 4-nitrophenolate is attributed, in part, to increased electron density at the binding site because of resonance delocalization of charge onto the nitro group. An analogous situation may exist for the anionic TNP-Ado: $\gamma$ -CD complex, where the negative charge is also delocalized onto the nitro groups of the TNP moiety, resulting in enhanced binding.

Large negative entropy changes typically arise from significantly reduced translational and conformational freedom of the cyclodextrin and the guest, while large negative enthalpy changes arise from van der Waals interactions due to complementary size and shape of the CD and guest.<sup>37</sup> Given that  $\alpha$ -CD and  $\beta$ -CD have much less effect on fluorescence enhancement,

(33) Connors, K. A. *Chem. Rev.* **1997**, *97*, 1325–1358.

(34) Rekharsky, M. V.; Inoue, Y. *Chem. Rev.* **1998**, *98*, 1875–1918.

(35) Liu, L.; Yang, C.; Guo, Q.-X. *Bull. Chem. Soc. Jpn.* **2001**, *74*, 2311–2314.

(36) Connors, K. A. *J. Pharm. Sci.* **1995**, *84*, 843–848.

(37) Rekharsky, M. V.; Inoue, Y. *J. Am. Chem. Soc.* **2002**, *124*, 813–826.

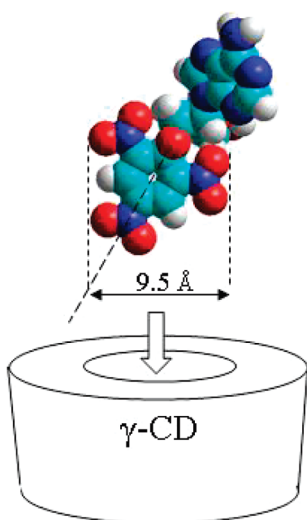


**FIGURE 8.** Optimized model of TNP-Ado anion (AM1) showing possible mode of insertion into the  $\gamma$ -CD cavity. The minimum CD diameter required for insertion is 9.5 Å, which matches the calculated diameter of  $\gamma$ -CD.<sup>38</sup>

the cavity size of the cyclodextrin appears to be critical for fluorescence enhancement of TNP-Ado. Molecular electrostatic potentials (MESP) have been derived by others for CDs utilizing hybrid density functional calculations.<sup>38</sup>  $\alpha$ -CD has a cone-like structure with primary and secondary rim diameters of 4.3 and 6.6 Å.  $\beta$ -CD and  $\gamma$ -CD have a more barrel-like structure with equal primary and secondary rim diameters, being 7.6 and 9.5 Å, respectively. An optimized model of the TNP-Ado anion (AM1), shown in Figure 8, reveals that a minimum CD diameter of  $\sim$ 9.5 Å is required for insertion of the TNP moiety, closely matching the rim diameter of  $\gamma$ -CD. Such inclusion would require insertion at an angle of  $\sim$ 30° relative to the symmetry axis of the TNP moiety, as shown in Figure 8. Slight twisting of the nitro groups may also occur upon insertion to provide an optimum stabilization of the complex. The good size–shape match of  $\gamma$ -CD and TNP-Ado accounts for the large negative enthalpy and entropy values experimentally determined in this study.

The fundamental mechanism(s) of enhanced TNP-Ado fluorescence by  $\gamma$ -CD has not been established. It is not uncommon that quantum yield increases when a fluorophore is bound to a biomolecule as in the case of TNP-ATP. In some instances, fluorescence can be attributed to restricted rotation of a particular bond of the fluorophore in the bound state. The nitro group specifically is known to undergo bond rotation (twisting) in the excited state of some aromatic systems, where the nitro group is orthogonal to the aromatic ring. The twisted conformation has been shown to be non-fluorescent in several systems due to a nonradiative pathway to the ground state.<sup>39–41</sup> The TNP-Ado Meisenheimer complex may exhibit restricted rotation of its nitro groups when bound to  $\gamma$ -CD, attributed to its tight insertion into the

hydrophobic cavity of  $\gamma$ -CD, resulting in enhanced fluorescence.

### 3. Conclusions

The ability of  $\gamma$ -CD to dramatically enhance fluorescence of the trinitrophenylated derivative of adenosine has been demonstrated. Kinetic and thermodynamic parameters were determined by using a combination of fluorimetry and NMR 2D EXSY spectroscopy. The complexation process is shown to be exclusively enthalpy-driven, with large negative entropy of complexation. These kinetic and thermodynamic characteristics could be taken into account to further optimize analysis of adenosine by capillary electrophoresis/laser-induced fluorescence detection (see the Supporting Information, Figures S-17 and S-18). The mode of TNP-Ado insertion has not been proven, but size–shape considerations strongly suggest that the TNP moiety inserts into the  $\gamma$ -CD cavity, resulting in enhanced fluorescence. Future studies will be required to elucidate the mechanism of fluorescence enhancement and the precise structure of the TNP-Ado: $\gamma$ -CD complex.

### 4. Experimental Section

**4.1. Materials.** All chemicals were reagent grade. Trinitrobenzenesulfonic acid (TNBS) should be handled with gloves in a fume hood. It should not be allowed to dry out, as it is potentially explosive when dry. Picric acid is a minor byproduct of the reaction with adenosine and base, and it is also potentially explosive when dry.

**4.2. Preparation of TNP-Ado, Li Salt.** A procedure similar to that of Hiratsuka was followed.<sup>9</sup> Adenosine (Ado, 30 mg, 0.11 mol) was added to 1 mL of water. TNBS (0.44  $\mu$ L, 0.44 mmol, 1 M in water) was added and the pH was adjusted to 10.0 with 1 M LiOH. More base was added over a 3 h period to maintain a pH of 10.0, and the reaction was left overnight. An aliquot was added to DMSO-*d*<sub>6</sub> and a <sup>1</sup>H spectrum was obtained to assess conversion. More base was added until integration revealed better than 98% conversion of Ado to TNP-Ado. The TNP-Ado solution was added to a Sephadex LH-20 column (1 cm  $\times$  5 cm) and eluted with  $\sim$ 20 mL of water. A pale yellow band eluted and a reddish-orange band (TNP-Ado) was retained at the top of the column. TNP-Ado was then eluted with about 20 mL of methanol. Methanol was removed under a flow of nitrogen and the TNP-Ado was used without further purification: 56% <sup>1</sup>H NMR <sup>13</sup>  $\delta$  DMSO-*d*<sub>6</sub> 8.70 (d, *J* = 3.1 Hz, 1H, H-3'' or H-5''), 8.50 (d, *J* = 3.1 Hz, 1H, H-3'' or H-5''), 8.43 (s, 1H, H-8), 8.15 (s, 1H, H-2), 7.33 (s, 2H, NH<sub>2</sub>), 6.38 (d, *J* = 3.1 Hz, 1H, H-1'), 5.41 (dd, *J* = 3.1, 8.1 Hz, 1H, H-2') 5.24 (dd, *J* = 8.1, 3.5 Hz, H-3'), 5.14 (t, *J* = 5.72 Hz, 1H, CH<sub>2</sub>OH), 4.42 (m, 1H, H-4'), 3.64 (m, 2H, H-5'); UV 408, 476 nm.

**4.3. Fluorescence Measurements and Quantum Yields.** Fluorescence measurements were carried out with excitation at 408 or 476 nm with a slit bandwidth of 2.5 nm. Emission was collected over a range of 460–640 nm with a slit bandwidth of 2.5 nm. The collection rate ranged from 20 to 100 nm/min. UV–vis absorbance spectra were also obtained with a 2.5 nm slit bandwidth. Quantum yield was estimated by using standard methods with fluorescein sodium salt in water as a standard (QY = 0.97) and excitation at 476 nm. Equilibrium constants were determined on a series of aqueous solutions containing 10  $\mu$ M TNP-Ado with varying concentrations of  $\gamma$ -CD (0.1–2.0 mM). Equilibrium data were fit with LabFit<sup>42</sup> curve fitting software,

(38) Pinjari, R. V.; Joshi, K. A.; Gejji, S. P. *J. Phys. Chem. A* **2006**, *110*, 13073–13080.

(39) Lapouyade, R.; Kuhn, A.; Letard, J.-F.; Rettig, W. *Chem. Phys. Lett.* **1993**, *208*, 48–58.

(40) Malval, J.-P.; Morlet-Savary, F.; Chaumeil, H.; Balan, L.; Versace, D.-L.; Jin, M.; Defoin, A. *J. Phys. Chem. C* **2009**, *113*, 20812–20821.

(41) Mondal, J. A.; Sarkar, M.; Samanta, A.; Ghosh, H. N.; Palit, D. K. *J. Phys. Chem. A* **2007**, *111*, 6122–6126.

(42) Silva, W. P.; Silva, C.M.D.P.S. LAB Fit Curve Fitting Software (Nonlinear Regression and Treatment of Data Program) V 7.2.47, **1999–2010**.

using a simple 1:1 complexation model and the Levenberg–Marquardt algorithm.

**4.4.  $^1\text{H}$ , EXSY, and ROESY NMR Spectra.**  $^1\text{H}$  NMR spectra were obtained at 300 MHz. Temperature-dependent  $^1\text{H}$  NMR spectra were referenced to  $\text{D}_2\text{O}$  according to its known variation of chemical shift with temperature.<sup>43</sup> Two-dimensional exchange (2D EXSY) spectra were recorded with the standard NOESY pulse sequence and the method of phase cycling described by States et al.<sup>44</sup> The spectra were collected into 512 data points in each block with quadrature detection, using a spectral width of 2012 Hz and mixing times ranging from 20 to 220 ms. Typically 128 t1 experiments were collected with 8 scans signal averaged for each t1 value. The recycle time was 2 s. The data were zero-filled in both dimensions to give  $1024 \times 1024$  real data points. Gaussian apodization was imposed in each dimension prior to Fourier transformation.

EXSY spectra were obtained on a 1.67:1 mixture of TNP-Ado and  $\gamma$ -CD (4.0 mM; 2.4 mM) in  $\text{D}_2\text{O}$  at temperatures of 10–20 °C. Under this condition,  $\gamma$ -CD is mostly complexed, thus a ~1:1 ratio of uncomplexed and complexed TNP-Ado exists. Data were fit to according to the equation:<sup>32</sup>

$$t_m = k[\ln(r+1)/(r-1)] \quad (3)$$

where  $k$  is the exchange rate constant,  $k = k'_1 + k'_{-1}$ ,  $t_m$  is the mixing time in seconds, and  $r$  is given by

$$r = 4X_A X_B (I_{AA} + I_{BB}) / (I_{AB} + I_{BA}) - (X_A - X_B)^2 \quad (4)$$

where  $X_A$  and  $X_B$  are the mole fractions of uncomplexed TNP-Ado and complexed TNP-Ado, respectively,  $I_{AA}$  and  $I_{BB}$  are

diagonal peak volumes, and  $I_{AB}$  and  $I_{BA}$  are crosspeak peak volumes. The rate constants  $k'_1$  and  $k'_{-1}$  are both pseudo-first-order rate constants for complexation and dissociation. The H-1' absorption of the ribose ring system was analyzed where the H-1' hydrogens of uncomplexed and complexed TNP-Ado appear as broad singlets at 6.1 and 6.3 ppm, with well-resolved diagonal and crosspeaks. A plot of  $t_m$  versus  $\ln[(r+1)/(r-1)]$  yields a straight line with slope of  $k$ . The standard error in  $k$  was estimated from the scatter of points about the line. At least 5 mixing times,  $t_m$ , were used at each temperature. Activation parameters were calculated according to the Eyring equation by plotting  $\ln(k/T)$  vs  $1/T$ , where the slope is  $-\Delta H^\ddagger/R$  and the intercept is  $\ln(k_B/h) + \Delta S^\ddagger/R$ , where  $\Delta H^\ddagger$  is the activation enthalpy,  $-\Delta S^\ddagger$  is the activation entropy,  $k_B$  is the Boltzmann constant,  $h$  is the Planck constant, and  $R$  is the gas constant.

Two-dimensional ROESY spectra were recorded on 1:1 mixtures of TNP-Ado and cyclodextrin (~5 mM each) with the standard ROESY pulse sequence and the method of phase cycling described by States et al.<sup>44</sup> The spectra were collected into 1024 data points in each block with quadrature detection by using a spectral width of 3000 Hz and mixing time of 200 ms. Typically 256 t1 experiments were collected with 32 scans signal averaged for each t1 value. The recycle time was 1.5 s. The data were zero-filled in both dimensions to give  $2048 \times 2048$  real data points. Gaussian apodization was imposed in each dimension prior to Fourier transformation.

**Supporting Information Available:**  $^1\text{H}$  NMR, EXSY, ROESY, van't Hoff plot, Job plot, Eyring plot, and double reciprocal plots. This material is available free of charge via the Internet at <http://pubs.acs.org>.

(43) Gottlieb, H. E.; Kotlyar, V.; Nudelman, A. *J. Org. Chem.* **1997**, *62*, 7512–7515.

(44) States, D. J.; Haberkorn, R. A.; Ruben, D. J. *J. Magn. Reson.* **1982**, *48*, 286–292.